

Received March 24, 2022, accepted March 30, 2022, date of publication April 4, 2022, date of current version April 15, 2022.

Digital Object Identifier 10.1109/ACCESS.2022.3164734

# An Adaptive Tunicate Swarm Algorithm for Optimization of Shallow Foundation

AMIRBAHADOR ARABALI<sup>1</sup>, MOHAMMAD KHAJEHZADEH<sup>2</sup>,  
SURAPARB KEAWSAWASVONG<sup>3</sup>, ADIL HUSSEIN MOHAMMED<sup>4</sup>,  
AND BASEEM KHAN<sup>5</sup>, (Senior Member, IEEE)

<sup>1</sup>Department of Civil Engineering, Faculty of Engineering, Central Tehran Branch, Islamic Azad University, Tehran 19558-47881, Iran

<sup>2</sup>Department of Civil Engineering, Anar Branch, Islamic Azad University, Anar 77419-43615, Iran

<sup>3</sup>Department of Civil Engineering, Thammasat School of Engineering, Thammasat University, Rangsit, Pathumthani 12120, Thailand

<sup>4</sup>Department of Communication and Computer Engineering, Faculty of Engineering, Cihan University-Erbil, Erbil, Kurdistan Region 44001, Iraq

<sup>5</sup>Department of Electrical Engineering, Kerman Branch, Islamic Azad University, Kerman 7635168111, Iran

Corresponding authors: Baseem Khan (baseem.khan04@gmail.com) and Mohammad Khajehzadeh (mohammad.khajehzadeh@gmail.com)

**ABSTRACT** This paper aims to introduce an adaptive metaheuristic algorithm based on tunicate swarm optimization (TSA) for effectively solving global optimization problems and the optimum design of a shallow spread foundation. The proposed adaptive tunicate swarm optimization (ATSA) has two main phases at each iteration: searching all around the search space based on a randomly selected tunicate and improving the search using the position of the best tunicate. This modification improves the algorithm's exploration ability while also preventing premature convergence. The suggested algorithm's performance is confirmed using a set of 23 mathematical test functions of well-known CEC 2017 and the outcomes are compared with TSA as well as some effective optimization algorithms. In addition, the new method automates the optimum design of shallow spread foundations while taking two objectives into account: cost and CO<sub>2</sub> emissions. The analysis and design procedures are based on both geotechnical and structural limit states. A case study of a spread foundation has been solved using the proposed methodology, and a sensitivity analysis has been conducted to investigate the effect of soil parameters on the total cost and embedded CO<sub>2</sub> emissions of the foundation. The simulation results demonstrate that, when compared to other competing algorithms, ATSA is superior and may produce better optimal solutions.

**INDEX TERMS** Tunicate swarm, metaheuristic, shallow foundation, cost, CO<sub>2</sub> emissions.

## I. INTRODUCTION

Many real-world design problems can be considered optimization problems, and an appropriate optimization method is required for the solution. On the other hand, design problems have become more complicated when discontinuities, incomplete information, dynamicity, and uncertainties are involved. In such a case, classical optimization algorithms based on mathematical principles demand exponential time or may not find the optimal solution at all. To overcome the mentioned problem, during the last few decades, introducing new efficient metaheuristic optimization algorithms to deal with the drawbacks of classical techniques has been of great concern. The privileges of these algorithms include derivation-free mechanisms, simple concepts and structure, local optima avoidance, and effectiveness for discrete and

continuous functions. Accordingly, there is an increasing interest in presenting new metaheuristic algorithms that offer higher accuracy and efficiency in dealing with complex optimization problems.

Particle swarm optimization was proposed by Kennedy and Eberhart [1], ant colony optimization was introduced by Dorigo and Di Caro [2], harmony search was proposed by Geem *et al.* [3], firefly algorithm was suggested by Yang [4], gravitational search algorithm was introduced by Rashedi *et al.* [5], sine cosine algorithm was developed by Mirjalili [6], crow search algorithm was proposed by Askarzadeh [7], spotted hyena optimizer was introduced by Dhiman and Kumar [8], Harris hawks optimization was presented by Heidari *et al.* [9], emperor penguin optimizer was proposed by Dhiman and Kumar [10], chameleon swarm algorithm was developed by Braik [11], sooty tern optimization algorithm was proposed by Dhiman and Kuar [12], hunter-prey optimization was developed by

The associate editor coordinating the review of this manuscript and approving it for publication was Bilal Alatas<sup>1</sup>.

Naruei *et al.* [13], and rat swarm optimizer was introduced by Dhiman *et al.* [14].

Although metaheuristic methods can yield acceptable results, no algorithm can solve all optimization problems better than others. In addition, in most engineering optimization problems, the objective function is discontinuous and has a large number of design variables. As a result, several research projects have been carried out to enhance the original metaheuristic algorithms' performance and efficiency and apply them to engineering problems. Dhiman [15] introduced a hybrid bio-inspired metaheuristic optimization approach, namely the Emperor Penguin and Salp Swarm Algorithms for engineering problems. Eslami *et al.* [16] proposed improved particle swarm optimization with chaotic sequence for optimal location of the power system stabilizer. Bingol and Alatas [17] proposed chaotic league championship algorithms for complex benchmark functions. Kaveh *et al.* [18] applied a non-dominated sorting genetic algorithm to solve the performance-based multi-objective optimal design of steel moment-frame structures considering the initial cost and the seismic damage cost. Dhiman *et al.* [19] developed a novel binary emperor penguin optimizer for automatic feature selection. Li and Wu [20] proposed an improved slap swarm optimization for determining the crucial failure surface in slope stability evaluation. Temur [21] introduced a hybrid version of teaching learning-based optimization for the optimum design of cantilever retaining walls under seismic loads. Bardhan *et al.* [22] proposed a modified equilibrium optimizer for predicting soil compression index. For pile group foundation design, Chan *et al.* [23] used an automated optimal design method based on a hybrid genetic algorithm. Bingol and Alatas [24] proposed enhanced optics inspired optimization for real-world engineering problems. Kumar and Dhiman [25] presented a comparative study of fuzzy optimization through fuzzy number. Khajehzadeh *et al.* [26] proposed modified gravitational search algorithm for multi-objective optimization of foundation.

Shallow spread foundation, a geotechnical structure that transfers loads to the soil beneath it immediately and is one of the most significant and sensitive structural components, has received a lot of attention in recent studies. Structures' functionality can be jeopardized unless the effective loads are successfully sent to the earth by a well-designed foundation. As a result, the proper design of the spread foundation has received wide attention in recent investigations. Traditionally, in the design of spread foundations, initial assumed dimensions will be checked for all geotechnical and structural limit states. If the dimensions are unable to satisfy the limitations, they will be changed until all of the requirements are met. The construction cost is not taken into account throughout this time-consuming iterative procedure. In the optimum design of these structures, the dimensions that provide the minimum cost or weight and satisfy all the requirements are defined automatically. Actually, spread foundations are widely used and typically involve a large amount of material volume. In addition, a considerable

portion of the structure's cost is associated with the foundations, and the economical design of foundations is an essential concern for geotechnical engineers. Therefore, several optimum design approaches for spread foundations have already been developed, with the main goal of these studies being cost reduction. Wang and Kulhawy [27] devised a design technique that took construction economics into account directly, resulting in a foundation with the lowest possible construction cost. Nigdeli *et al.* [28] employed three metaheuristic optimization algorithms, including Flower Pollination Algorithm, Harmony Search and Teaching-Learning Based Optimization algorithm for the optimum design of reinforced concrete footings. Gandomi and Kashani [29] considered the final cost of foundation as an objective function and applied eight swarm intelligence techniques to the problem. Kashani *et al.* [30] investigated the performance of three evolutionary algorithms, namely, evolution strategy, differential algorithm, and biogeography-based optimization algorithm for foundation design optimization.

On the other hand, as the annual emissions of carbon dioxide (CO<sub>2</sub>) have grown by up to 80% since 1970, the consideration of CO<sub>2</sub> emissions in the design of concrete structures has become of greater interest among researchers. The main binder used in concrete is Portland cement, and a large amount of CO<sub>2</sub> is produced during its manufacturing. Therefore, minimization of embedded CO<sub>2</sub> emissions seems crucial to incorporate into the design criteria of reinforced concrete structures. For optimization of embedded carbon dioxide (CO<sub>2</sub>) emissions and the economic cost of reinforced concrete walls, Yepes *et al.* [31] suggested a hybrid optimization method based on a variable neighborhood search threshold acceptance strategy. Paya-Zaforteza *et al.* [32] implemented the well-known simulated annealing (SA) algorithm to design reinforced concrete (RC) building frames with the lowest possible embedded CO<sub>2</sub> emissions and the lowest possible RC frame construction cost. Using a hybrid glowworm swarm optimization algorithm, Yepes *et al.* [33] developed a way for optimizing cost and CO<sub>2</sub> emissions while designing precast-prestressed concrete road bridges with a double U-shape cross-section. Khajehzadeh *et al.* [34] developed an effective hybrid evolutionary approach based on an adaptive gravitational search algorithm for multi-objective optimization of reinforced concrete (RC) retaining walls.

Recently, Kaur *et al.* [35] suggested the tunicate swarm algorithm (TSA) as a new bioinspired meta-heuristic optimization technique. Tunicates use swarm intelligence and jet propulsion at sea to choose the optimal state for seeking food in their surroundings. TSA outperforms other competitor approaches when it comes to identifying optimal solutions and is well-suited to real-world optimization challenges. Sharma *et al.* [36] applied TSA for parameter extraction of the photovoltaic module. Li *et al.* [37] developed an improved version of the tunicate swarm algorithm (ITSA) for solving and optimizing the dynamic economic emission dispatch (DEED) problem. Fetouh and Elsayed [38] proposed an improved tunicate swarm algorithm for optimal control

and operation of fully automated distribution networks. Rizk-Allah et al. [39] applied an enhanced TSA for solving large-scale nonlinear optimization problems. Al-Wesabi et al. [40] developed a multi-objective quantum tunicate swarm optimization with a deep learning model for intelligent dystrophinopathy diagnosis. Mansoor et al. [41] proposed an intelligent tunicate swarm algorithm for multiple configurations of Photovoltaic systems under partial shading conditions. Khajehzadeh et al. [42] developed a hybrid version of TSA for seismic analysis of earth slopes. Houssein et al. [43] presented an improved tunicate swarm algorithm for global optimization and image segmentation.

However, it is prone to becoming stuck in local optima and is unable to find the optimal answer in some difficult circumstances [44].

In order to overcome this weakness, in the current study, an adaptive version of the tunicate swarm algorithm (ATSA) is developed and utilized for spread foundation optimization. Therefore, the main contribution of this work can be summarized as follows:

- 1- An effective global optimization algorithm (ATSA) based on the tunicate swarm algorithm has been developed.
- 2- Two separate phases are introduced in the TSA to increase both the global and local search capability of the original algorithm.
- 3- The performance of ATSA is evaluated on 23 frequently used benchmark functions and compared to other optimization algorithms.
- 4- To verify the effectiveness of the proposed method for the solution of real-world problems, the new method is applied to spread foundation optimization.
- 5- In the optimum design of the foundation, total construction cost as well as total CO<sub>2</sub> emissions are considered as objective functions.

## II. FOUNDATION OPTIMIZATION

Reinforced spread foundation, as a key geotechnical construction, must securely and reliably support the superstructure, maintain stability against excessive settlement and failure of the soil's bearing capacity, and restrict concrete stresses. Aside from these design goals, spread foundations must meet a number of requirements. In both long and short dimensions, they must have sufficient shear and moment capacities, and the steel reinforcement design must comply with all design codes.

Mathematically, general form of a constraint optimization problem can be expressed as follows:

$$\begin{aligned}
 & \text{minimize } f(\mathbf{X}) \\
 & \text{subject to } g_i(\mathbf{X}) \leq 0, \quad i = 1, 2, \dots, p, \quad (1) \\
 & \quad \quad h_j(\mathbf{X}) = 0, \quad j = 1, 2, \dots, m, \\
 & \quad \quad \mathbf{X}^L \leq \mathbf{X} \leq \mathbf{X}^U
 \end{aligned}$$

where  $\mathbf{X}$  is  $n$  dimensional vector of design variables,  $f(\mathbf{X})$  is the objective function,  $g(\mathbf{X})$  and  $h(\mathbf{X})$ , respectively, are inequality and equality constraints. Boundary constraints,

$\mathbf{X}^L$  and  $\mathbf{X}^U$ , are two  $n$ -dimensional vectors containing the design variables' lower and upper bounds, respectively.

In the problem of foundation optimization, it is required to identify the objective function, design constraint, and design variables that are presented in the following sub-sections.

### A. OBJECTIVE FUNCTION

In the current study, the problem of spread foundation optimization considers the embedded CO<sub>2</sub> emission and the construction cost of the structure. Hence, this optimization problem aims to minimize one of these two objective functions. Both objective functions consider the amount of excavation, formwork, reinforcing steel, concrete, and compacted backfill.

The total cost of the structure is presented in the following equation:

$$f_{cost} = C_s W_{st} + C_c V_c + C_e V_e + C_f A_f + C_b V_b \quad (2)$$

where,  $W_{st}$  is the weight of the steel bars,  $V_c$ ,  $V_e$  and  $V_b$  denote the volume of concrete, excavation and backfill.  $A_f$  shows the area of formwork.  $C_c$ ,  $C_e$ ,  $C_b$ ,  $C_f$  and  $C_s$  are the unit costs of concrete, excavation, backfill, formwork, and reinforcement, respectively. The unit prices are presented in Table 1 [45].

The next objective which quantify the total amount of CO<sub>2</sub>-emissions of the footing can be expressed in the following form:

$$f_{CO_2} = E_s W_{st} + E_c V_c + E_e V_e + E_f A_f + E_b V_b \quad (3)$$

where,  $E_c$ ,  $E_e$ ,  $E_b$ ,  $E_f$  and  $E_s$  are the unit emission of concrete, excavation, backfill, formwork, and reinforcement, respectively as presented in Table 1 [45].

TABLE 1. Unit cost and CO<sub>2</sub> emission of foundation construction [45].

Item	Unit	Symbol	Value
Cost of earth removal	\$/m <sup>3</sup>	$C_e$	25.16
Cost of foundation formwork	\$/m <sup>2</sup>	$C_f$	51.97
Cost of reinforcement	\$/kg	$C_s$	2.16
Cost of concrete	\$/m <sup>3</sup>	$C_c$	173.96
Cost of compacted backfill	\$/m <sup>3</sup>	$C_b$	3.97
CO <sub>2</sub> emission for earth removal	kg/m <sup>3</sup>	$E_e$	13.16
CO <sub>2</sub> emission for foundation formwork	kg/m <sup>2</sup>	$E_f$	14.55
CO <sub>2</sub> emission for reinforcement	kg/kg	$E_s$	3.02
CO <sub>2</sub> emission for concrete	kg/m <sup>3</sup>	$E_c$	224.65
CO <sub>2</sub> emission for compacted backfill	kg/m <sup>3</sup>	$E_b$	27.20

### B. DESIGN VARIABLES

The design factors for the spread footing model are shown in Figure 1. There are two types of design variables: those that define geometrical parameters and those that describe reinforcing steel. The dimensions of the foundation are represented by four geometric design variables, as illustrated in

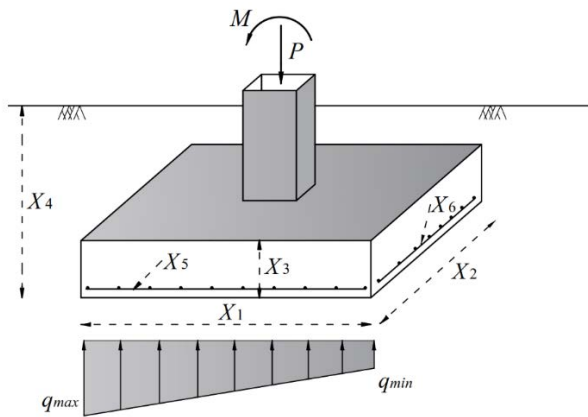


FIGURE 1. Design variables of the footing.

Figure 1.  $X_1$  is the foundation’s length,  $X_2$  is the foundation’s width,  $X_3$  is foundation’s thickness and  $X_4$  is depth of embedment. Moreover, the steel reinforcement has two design variables:  $X_5$  is the longitudinal reinforcement and  $X_6$  is the transverse reinforcement.

**C. DESIGN CONSTRAINTS**

The forces operating on the footing are depicted in Figure 1.  $M$  and  $P$  denote the axial load and moment imparted to the footing in this figure. The minimum and maximum bearing pressures on the foundation’s base are  $q_{min}$  and  $q_{max}$ , respectively. The next sub-sections go over the design restrictions that must be taken into account when optimizing the spread footing.

**1) BEARING CAPACITY**

The foundation’s bearing capacity must be sufficient to withstand the forces acting along the base. The maximum stress should be less than the soil’s bearing capacity to ensure a safe design:

$$q_{max} \leq \frac{q_{ult}}{FS} \tag{4}$$

where  $q_{ult}$  denotes the foundation’s ultimate bearing capacity and  $q_{max}$  is the maximum contact pressure at the boundary between the foundation’s bottom and the underlying soil. The lowest and highest applied bearing pressures on the foundation’s base are calculated as follows:

$$q_{min}^{max} = \frac{P}{X_1 X_2} \left( 1 \mp \frac{6e}{X_1} \right) \tag{5}$$

where  $e$  denotes the eccentricity, which is defined as the ratio of the overturning moments ( $M$ ) to the total vertical forces ( $P$ ).

**2) ECCENTRICITY**

The following requirements must be met such that tensile forces at the bottom of the footing are avoided:

$$e \leq \frac{X_1}{6} \tag{6}$$

**3) SETTLEMENT**

According to the following inequalities, foundation settlement should be kept within a legal range:

$$\delta \leq \delta_{all} \tag{7}$$

where  $\delta_{all}$  is the permitted settlement and  $\delta$  is the foundation’s immediate settlement. The settlement can be estimated as follows using the elastic solution proposed by Poulos and Davis [46]:

$$\delta = \frac{P(1 - \nu^2)}{\kappa_z E \sqrt{X_1 X_2}} \tag{8}$$

where  $\kappa_z$  is the shape factor,  $\nu$  is the Poisson’s ratio and  $E$  is modulus of elasticity. In this research, the shape factor proposed by Wang and Kulhawy [27] is used as follows:

$$\kappa_z = -0.0017(X_2/X_1)^2 + 0.0597(X_2/X_1) + 0.9843 \tag{9}$$

where,  $X_1$  is the foundation’s length, and  $X_2$  is the foundation’s width.

**4) ONE-WAY SHEAR**

The footing must be viewed as a wide beam for one-way shear. According to ACI [47], the shear strength of concrete measured along a vertical plane extending the whole width of the base and located at a distance equal to the effective depth of the footing ( $V_u$ ) should be less than nominal shear strength of concrete:

$$V_u \leq \frac{1}{6} \phi_v \sqrt{f'_c} b d \tag{10}$$

where  $\phi_v$  is the shear strength reduction factor of 0.75 [47],  $f'_c$  is the concrete compression strength,  $b$  is the section width, and  $d$  denotes the depth at which steel reinforcement is placed.

**5) TWO-WAY SHEAR**

The tendency of the column to punch through the footing slab is called “punching shear”. According to (11), the maximum shearing force in the upward direction ( $V_u$ ) should be less than the nominal punching shear strength to avoid such a failure.

$$V_u \leq \min \left\{ \frac{1 + \frac{2}{\beta_c}}{6}, \frac{\alpha_s d}{b_0} + 2, \frac{1}{3} \right\} \phi_v \sqrt{f'_c} b_0 d \tag{11}$$

where  $b_0$  is the crucial section’s perimeter taken at  $d/2$  from the column’s face,  $d$  denotes the depth at which steel reinforcement is placed,  $\beta_c$  is the ratio of a column section’s long side to its short side and  $\alpha_s$  is equal to 40 for interior columns.

6) BENDING MOMENT

The nominal flexural strength of the reinforced concrete foundation section should be less than the moment capacity [47]:

$$M_u \leq \phi_M A_s f_y \left( d - \frac{a}{2} \right) \tag{12}$$

where  $M_u$  denotes the bending moment of the reaction stresses due to the applied load at the column's face,  $\phi_M$  presents the flexure strength reduction factor equal to 0.9 [47],  $A_s$  denotes the area of steel reinforcement and  $f_y$  is the yield strength of steel.

7) REINFORCEMENTS LIMITATION

In each direction of the footing, the amount of steel reinforcement must fulfill minimum and maximum reinforcement area limitations according to the following inequality [47]:

$$\rho_{min} bd \leq A_s \leq \rho_{max} bd \tag{13}$$

where  $A_s$  is the cross section of steel reinforcement,  $\rho_{min}$  and  $\rho_{max}$  are the minimum and maximum reinforcement ratios based on the following equations [47]:

$$\rho_{min} = \max \left\{ \frac{1.4}{f_y}, 0.25 \frac{\sqrt{f'_c}}{f_y} \right\} \tag{14}$$

$$\rho_{max} = 0.85 \beta_1 \frac{f'_c}{f_y} \left( \frac{600}{600 + f_y} \right) \tag{15}$$

where,  $\beta_1$  is a constant equal to 0.85 [47].

8) LIMITATION OF EMBEDMENT'S DEPTH

The depth of embedment ( $X_4$ ) should be limited between 0.5 and 2. Therefore:

$$0.5 \leq X_4 \leq 2 \tag{16}$$

To address the above mentioned limitations and transform a constrained optimization to an unconstrained one, a penalty function method is used in this paper. according to:

$$F(X) = f(X) + r \sum_{i=1}^p \max\{0, g_i(X)\}^l \tag{17}$$

where  $F(X)$  is the penalized objective function,  $f(X)$  is the problem's original objective function presented in (2) and (3) and  $r$  is a penalty factor and  $p$  in the total number of constraints.

III. TUNICATE SWARM ALGORITHM (TSA)

TSA is a simple meta-heuristic optimizer inspired by the performance of marine tunicates and their jet propulsion systems during navigation and foraging. [35]. This animal has a millimeter-scale form. Tunicate can locate food sources in the sea. In the supplied search space, however, there is no indication of the food source. A tunicate must satisfy three basic conditions when traveling with jet propulsion: it must avoid colliding with other tunicates in the search space; it must take the correct path to the optimal search location; and it must be as close to the best search agent as possible. The candidate

solutions (i.e., tunicates) in TSA are looking for the best food source (i.e., the best value of the objective function). The tunicates change their positions in reference to the best tunicates that are stored and improved in each iteration during this process. The TSA starts with a population of randomly generated tunicates based on the design variables' allowable boundaries, as shown in the equation below:

$$\vec{T}_p = \vec{T}_p^{min} + rand \times (\vec{T}_p^{max} - \vec{T}_p^{min}) \tag{18}$$

where,  $\vec{T}_p$  is the position of each tunicate and  $rand$  is a random number within range [0, 1].  $\vec{T}_p^{min}$  and  $\vec{T}_p^{max}$  are design variables' lower and upper bounds, respectively. The tunicates adjust their location during the iterations by the following formula [35]:

$$\vec{T}_p(\vec{x} + 1) = \frac{\vec{T}_p(x) + \vec{T}_p(\vec{x})}{2 + c_1} \tag{19}$$

where,  $c_1$  is a random number within range [0,1] and  $\vec{T}_p(x)$  refers to the updated position of the tunicate with respect to the position of the food source based on (20).

$$\vec{T}_p(x) = \begin{cases} SF + A \times |SF - rand \times \vec{T}_p|, & \text{if } rand \geq 0.5 \\ SF - A \times |SF - rand \times \vec{T}_p|, & \text{if } rand < 0.5 \end{cases} \tag{20}$$

where  $SF$  is the food source, which is represented by the population's optimal tunicate position; and  $A$  denotes a randomized vector to prevent tunicates from colliding with one another which is modelled as:

$$A = \frac{c_2 + c_3 - 2c_1}{VT_{min} + c_1 (VT_{max} - VT_{min})} \tag{21}$$

where,  $c_1$ ,  $c_2$  and  $c_3$  are random numbers within range [0, 1];  $VT_{min}$  and  $VT_{max}$  reflect the minimum and maximum speeds that are used to create social interaction which considered as 1 and 4, respectively [35].

The TSA algorithm's steps are presented below:

Step 1: Initialize the tunicate population  $\vec{T}_p$  based on (18).

Step 2: Choose the initial parameters and maximum number of iterations.

Step 3: Calculate the fitness value of each search agent.

Step 4: The best tunicate is explored in the given search space.

Step 5: Update the position of each tunicate using (19).

Step 6: Adjust the updated tunicate which goes beyond the boundary in a given search space.

Step 7: Compute the updated tunicate fitness value. If there is a better solution than the previous optimal solution, then update the best.

Step 8: If the stopping criterion is satisfied, then the algorithm stops. Otherwise, repeat the Steps 5–8.

Step 9: Return the best optimal solution which is obtained so far.



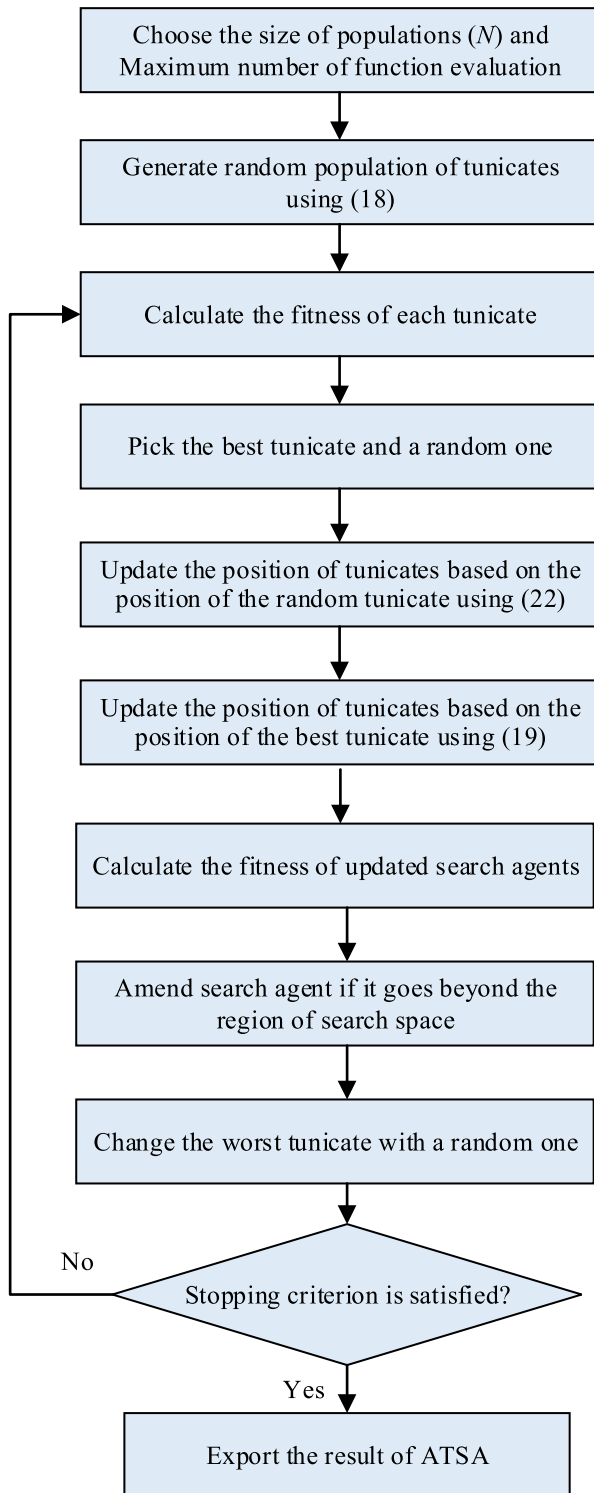


FIGURE 2. Flowchart of the ATSA.

IV. ADAPTIVE TUNICATE SWARM ALGORITHM

Despite the TSA’s ability to produce efficient results when compared to other well-known algorithms, it is susceptible to becoming trapped in local optima and is not ideal for very complex problems with several local optima [44]. As shown

in (19) and (20), in TSA, every tunicate updates its position based on the position of the food source (i.e., the position of the best tunicate in the whole population). However, without any knowledge of the position of the food source (FS), there will not be any recovery for the algorithm if premature convergence happens. In other words, once the algorithm has converged, it loses its potential to explore and becomes inactive. Therefore, the TSA algorithm becomes locked at local minimum points as a result of this mechanism. In light of these conditions, an adaptive version of the TSA (ATSA) is proposed to overcome the mentioned weaknesses and increase the search capability and flexibility of the algorithm.

An effective metaheuristic algorithm needs to divide the search process into two phases: exploration and exploitation. Exploration involves exploring new positions far from the current position in the entire search area. The exploration phase takes place when a metaheuristic algorithm attempts to identify the entire solution space and explore the promising areas. In contrast, exploitation refers to the capability of an optimization algorithm to search around near-optimal solutions. This phase allows the optimizer to concentrate on the neighborhood that consists of higher-quality solutions within the searching space. As mentioned earlier, at each iteration pass, the TSA algorithm updates the position of candidate solutions around a single point that is the best solution in the whole population. It means the TSA has a good exploitation capability. However, its weakness is the lack of an effective global search and the algorithm suffers from an effective exploration ability.

In order to improve the performance and exploration capability of the algorithm, the proposed ATSA has two main phases in each iteration. In the first phase (exploration phase), a candidate solution is picked at random instead of the best solution, and the position of the candidate solutions will be updated according to the position of this random tunicate. In addition, to have effective exploration, an optimizer should use its randomized operators to thoroughly explore diverse areas of the search space [9]. Therefore, in the proposed ATSA, two separate random numbers are considered in the tunicate’s updating equation to produce solutions in various regions of the search space.

The exploration phase of the ATSA is mathematically modeled as follows:

$$\vec{T}_p(\vec{x} + 1) = \vec{T}_p(r) - rand_1 \times |\vec{T}_p(r) - 2 \times rand_2 \times \vec{T}_p(\vec{x})| \tag{22}$$

where  $\vec{T}_p(r)$  is randomly selected tunicate form the current population.  $rand_1$  and  $rand_2$  are random numbers between 0 and 1. This procedure promotes exploration and also allows the TSA algorithm to perform a more robust global search throughout the whole search space.

In the second phase of the ATSA algorithm (exploitation phase), the tunicates update their positions according to the position of the best tunicate found so far, based on (19).

TABLE 2. Description of unimodal benchmark functions.

Function	Name [48]	Range	$f_{min}$	$n$ (Dim)
$F_1(X) = \sum_{i=1}^n x_i^2$	Sphere function	$[-100, 100]^n$	0	30
$F_2(X) = \sum_{i=1}^n  x_i  + \prod_{i=1}^n  x_i $	Schwefel's problem 2.22	$[-10, 10]^n$	0	30
$F_3(X) = \sum_{i=1}^n \left( \sum_{j=1}^i x_j \right)^2$	Schwefel's problem 1.2	$[-100, 100]^n$	0	30
$F_4(X) = \max_i \{  x_i , 1 \leq i \leq n \}$	Schwefel's problem 2.21	$[-100, 100]^n$	0	30
$F_5(X) = \sum_{i=1}^{n-1} [100(x_{i+1} - x_i^2)^2 + (x_i - 1)^2]$	Generalized Rosenbrock's function	$[-30, 30]^n$	0	30
$F_6(X) = \sum_{i=1}^n ((x_i + 0.5))^2$	Step function	$[-100, 100]^n$	0	30
$F_7(X) = \sum_{i=1}^n ix_i^4 + random[0,1)$	Quartic function with noise	$[-1.28, 1.28]^n$	0	30

Furthermore, in the proposed ATSA, the worst tunicate with the highest objective function value will be replaced with a randomly generated tunicate at each iteration. Figure 2 shows the flowchart of the proposed ATSA algorithm.

**A. COMPARATIVE TIME COMPLEXITY ANALYSIS**

In order to evaluate the overall performance of a new optimization algorithm from different points of view, the computational time complexity analysis can be conducted. In computer sciences, the ‘‘Big O notation’’ is a mathematical notation which represents the required running time of an algorithm by considering the growth rate in dealing with different inputs.

The time complexity analysis of most algorithms involves analyses of three components. Likewise, the time complexity analysis of the proposed ATSA also requires analyses of these three components:

1. Time complexity of initialization of the population, generally calculated by  $O(N \times D)$  where  $N$  denotes the population size and  $D$  denotes the dimensions of the problem.
2. Time complexity of initial fitness evaluation, generally evaluated by  $O(N \times F(X))$ , where  $F(X)$  represents the objective function.
3. Time complexity of the main loop, generally calculated by  $O(Maxiterations \times (N \times D + N \times F(X)))$ , where  $Maxiterations$  is the maximum number of iterations.

Hence, the total time complexity of ATSA algorithm is  $O(Maxiterations (N \times D + N \times F(X)))$ .

**V. PERFORMANCE EVALUATION OF THE ATSA**

The effectiveness of the suggested ATSA approach will be investigated in this section. To this aim, on a set of benchmark test functions from the literature, the performance of the new method is compared to that of the standard version of the algorithm (TSA) as well as some well-known

metaheuristic algorithms. These are all minimization problems that can be used to test the new optimization algorithms’ robustness and exploration efficiency. The mathematical description and characteristics of these test functions are shown in Tables 2, 3, 4. This benchmark set covers three main groups: unimodal functions with a unique global best for testing the convergence speed and exploitation ability of the algorithms; multimodal functions with multiple local solutions and a global optimum for testing local optima avoidance and exploration capability of an algorithm; and finally multimodal functions with a fixed dimension.

The ATSA algorithm’s performance is compared with the original TSA and some efficient optimization methods, including Gravitational Search Algorithm (GSA), Grey Wolf Optimizer (GWO), and Sine Cosine Algorithm (SCA). It’s worth noting that the ATSA algorithm evaluates the objective function twice per iteration, whereas the TSA and other approaches do so just once. Therefore, according to the suggestion of the previous studies [35] and to have a fair comparison between the results, the size of the population ( $N$ ) is considered equal to 40 for ATSA and equal to 80 for TSA and other approaches. In addition, for all techniques, the maximum number of iterations is considered equal to 1000. In this way, in all experiments, the same number of function evaluations, equal to 80,000, is used. The results of a single run may be incorrect since metaheuristic approaches are stochastic. As a result, to generate a meaningful comparison and evaluate the effectiveness of the algorithms, a statistical analysis should be utilized. To address this issue, 30 independent runs for the stated algorithms are performed, with the results presented in Tables 5, 6, 7.

The results of Tables 5, 6, 7, show the best (minimum), worst (maximum), mean (average), median and standard deviation (Std) of the solutions obtained from experiments using the selected optimization algorithms. The best results

TABLE 3. Description of multimodal benchmark functions.

Function	Name [48]	Range	$f_{min}$	$n$ (Dim)
$F_8(X) = \sum_{i=1}^n -x_i \sin(\sqrt{ x_i })$	Generalized Schwefel's problem 2.26	$[-500, 500]^n$	$428.9829 \times n$	30
$F_9(X) = \sum_{i=1}^n [x_i^2 - 10 \cos(2\pi x_i) + 10]$	Generalized Rastrigin's function	$[-5.12, 5.12]^n$	0	30
$F_{10}(X) = -20 \exp\left(-0.2 \sqrt{\frac{1}{n} \sum_{i=1}^n x_i^2}\right) - \exp\left(\frac{1}{n} \sum_{i=1}^n \cos(2\pi x_i)\right) + 20 + e$	Ackley's function	$[-32, 32]^n$	0	30
$F_{11}(X) = \frac{1}{4000} \sum_{i=1}^n x_i^2 - \prod_{i=1}^n \cos\left(\frac{x_i}{\sqrt{i}}\right) + 1$	Ackley's function	$[-600, 600]^n$	0	30
$F_{12}(X) = \frac{\pi}{n} \left\{ 10 \sin(\pi y_1) + \sum_{i=1}^{n-1} (y_i - 1)^2 [1 + 10 \sin^2(\pi y_{i+1})] + (y_n - 1)^2 \right\} + \sum_{i=1}^n u(x_i, 10, 100, 4)$ $y_i = 1 + \frac{x_{i+4}}{4}$ $u(x_i, a, k, m) = \begin{cases} k(x_i - a)^m & x_i > a \\ 0 & a < x_i < -a \\ k(-x_i - a)^m & x_i < -a \end{cases}$	Generalized penalized function	$[-50, 50]^n$	0	30
$F_{13}(X) = 0.1 \left\{ \sin^2(3\pi x_1) + \sum_{i=1}^n (x_i - 1)^2 [1 + \sin^2(3\pi x_i + 1)] + (x_n - 1)^2 [1 + \sin^2(2\pi x_n)] \right\} + \sum_{i=1}^n u(x_i, 5, 100, 4)$	Generalized penalized function	$[-50, 50]^n$	0	30

among the five algorithms are shown in bold. According to the results of these tables in the following subsections, the exploration, exploitation, and convergence rate of the new method are investigated using a comparative performance comparison of ATSA against four selected algorithms.

**A. EXPLOITATION CAPABILITY**

Unimodal test functions can be considered to investigate the exploitation capability of an optimization algorithm [49], [50]. In this study, to evaluate the ability of ATSA to exploit the promising regions, seven unimodal benchmark functions ( $F_1$  to  $F_7$ ) are solved and the results are compared with four selected optimization methods in Table 5. The results of this table show that, for all unimodal functions except  $F_6$ , ATSA could provide a better solution. In addition, for four functions ( $F_1$ - $F_4$ ), ATSA reached the global optima. It means that the new algorithm has a large potential search space compared with the other optimization algorithms.

**B. EXPLORATION VERIFICATION**

In order to evaluate the capability of an optimization algorithm to effectively explore the search space, multimodal benchmark functions that have many local optima are usually considered [49], [50]. Based on the presented procedure,

16 multimodal functions ( $F_8$  to  $F_{23}$ ) are minimized. According to the results of Tables 6 and 7, it can be observed that the best and mean values reached by ATSA for most of the functions (except  $F_{13}$ ) are significantly better than the other methods. However, for  $F_{13}$ , the results are also comparable to the other algorithms. From the standard deviation point of view, which indicates the stability of the algorithm, the results show that ATSA is a more stable method when compared with the other techniques. From the analysis, it can be concluded that ATSA either outperforms the other algorithms or performs almost equivalently. The consistent performance of the new method for such a comprehensive suite of multimodal benchmark functions verifies its superior capabilities of exploration.

**C. CONVERGENCE CAPABILITY**

The convergence progress curves of ATSA for benchmark test functions are compared with TSA, GSA, SCA, and GWO in Figure 3. The curves are plotted against the number of function evaluations. The descending trend is quite evident in the convergence curve of ATSA on all of the test functions investigated. This strongly evidences the ability of the new algorithm to obtain a better approximation of the global optimum over the course of iterations. In addition, the curves of test functions show that ATSA is capable of exploring the



TABLE 4. Description of fixed-dimension multimodal benchmark functions.

Function	Name [48]	Range	$f_{min}$	$n$ (Dim)
$F_{14}(X) = \left( \frac{1}{500} + \sum_{j=1}^{25} \frac{1}{j + (x_i - a_{ij})^6} \right)^{-1}$	Shekel's Foxholes function	$[-65.53, 65.53]^n$	1	2
$F_{15}(X) = \sum_{i=1}^{11} \left[ a_i - \frac{x_1(b_i^2 + b_i x_2)}{b_i^2 + b_i x_3 + x_4} \right]^2$	Kowalik's function	$[-5, 5]^n$	0.00030	4
$F_{16}(X) = 4x_1^2 - 2.1x_1^4 + \frac{1}{3}x_1^6 + x_1x_2 - 4x_2^2 + 4x_2^4$	Six-hump camel back function	$[-5, 5]^n$	-1.0316	2
$F_{17}(X) = \left( x_2 - \frac{5.1}{4\pi^2}x_1^2 + \frac{5}{\pi}x_1 - 6 \right)^2 + 10 \left( 1 - \frac{1}{8\pi} \right) \cos x_1 + 10$	Branin function	$[-5, 5]^n$	0.398	2
$F_{18}(X) = [1 + (x_1 + x_2 + 1)^2(19 - 14x_1 + 3x_1^2 - 14x_2 + 6x_1x_2 + 3x_2^2)] \times [30 + (2x_1 - 3x_2)^2] \times [(18 - 32x_1 + 12x_1^2 + 48x_2 - 36x_1x_2 + 27x_2^2)]$	Goldstein-Price function	$[-2, 2]^n$	3	2
$F_{19}(X) = -\sum_{i=1}^4 c_i \exp \left( -\sum_{j=1}^3 a_{ij}(x_j - p_{ij}) \right)^2$	Hartman's family	$[1, 3]^n$	-3.86	3
$F_{20}(X) = -\sum_{i=1}^4 c_i \exp \left( -\sum_{j=1}^6 a_{ij}(x_j - p_{ij}) \right)^2$	Hartman's family	$[0, 1]^n$	-3.32	6
$F_{21}(X) = -\sum_{i=1}^5 [(X - a_i)(X - a_i)^T + c_i]^{-1}$	Shekel's family	$[0, 10]^n$	-10.1532	4
$F_{22}(X) = -\sum_{i=1}^7 [(X - a_i)(X - a_i)^T + c_i]^{-1}$	Shekel's family	$[0, 10]^n$	-10.4028	4
$F_{23}(X) = -\sum_{i=1}^{10} [(X - a_i)(X - a_i)^T + c_i]^{-1}$	Shekel's family	$[0, 10]^n$	-10.5363	4

search space extensively and identifying the most promising region in fewer iterations. The obtained results indicate that the ATSA outperforms the other algorithms in most cases and has faster convergence to the best solution.

D. STATISTICAL SIGNIFICANCE ANALYSIS

In order to determine the statistical significance of the comparative results between two or more algorithms, a non-parametric pairwise statistical analysis should be conducted. As recommended by Derrac et al. [51], to assess meaningful comparison between the proposed and alternative methods, the nonparametric Wilcoxon's rank sum test is performed between the results. In this regard, utilizing the best results obtained from 30 runs of each method, a pair-wise comparison is conducted.

Wilcoxon's rank sum test returns  $p$ -value, sum of positive ranks ( $R+$ ) and the sum of negative ranks ( $R-$ ) [52]. Table 8 presents the results of Wilcoxon's rank sum test of ATSA when compared with other methods. The  $p$ -value indicates the minimum significance level for detecting differences. In this study,  $\alpha = 0.05$  is considered as the level of significance. If the  $p$ -value of the given algorithm is greater than 0.05, then there is no significant difference between the two compared methods. Such a result is indicated with "N.A" in the winner rows of Table 8. On the other hand, if the  $p$ -value is less than  $\alpha$ , it definitively means that, in each pair-wise comparison, the better result obtained by the best algorithm is statistically significant and was not gained by chance. In such cases, if the  $R+$  is bigger than  $R-$ , indicates ATSA has a superior performance than the alternative method otherwise

TABLE 5. Results comparison of unimodal test functions.

Fun.	Index	ATSA	TSA	SCA	GSA	GWO
F <sub>1</sub>	Best	<b>0.00</b>	5.1458e-61	1.5523e-07	1.001e-17	2.4915e-61
	Worst	<b>0.00</b>	1.1586e-54	0.0043	3.186e-17	3.8647e-58
	Mean	<b>0.00</b>	8.3155e-56	2.3458e-04	2.114e-17	4.9162e-59
	Median	<b>0.00</b>	7.1012e-58	1.9737e-05	2.007e-17	1.0534e-59
	Std.	<b>0.00</b>	2.4905e-55	7.9295e-04	5.815e-18	1.0230e-58
F <sub>2</sub>	Best	<b>0.00</b>	1.1196e-35	1.5605e-09	1.528e-08	8.3612e-36
	Worst	<b>0.00</b>	3.2814e-32	9.8446e-06	3.331e-08	5.3488e-34
	Mean	<b>0.00</b>	2.1532e-33	1.6882e-06	2.393e-08	8.3658e-35
	Median	<b>0.00</b>	3.1044e-34	5.4000e-07	2.346e-08	5.9294e-35
	Std.	<b>0.00</b>	6.0237e-33	2.4046e-06	4.002e-09	9.8594e-35
F <sub>3</sub>	Best	<b>0.00</b>	2.5684e-32	70.8285	102.955	1.2533e-19
	Worst	<b>0.00</b>	2.4492e-17	2.6762e+03	468.616	3.5572e-13
	Mean	<b>0.00</b>	8.1741e-19	789.1620	245.469	1.5096e-14
	Median	<b>0.00</b>	1.8696e-24	619.4506	221.115	2.0740e-17
	Std.	<b>0.00</b>	4.4714e-18	746.2287	100.102	6.5547e-14
F <sub>4</sub>	Best	<b>0.00</b>	3.2458e-08	1.2610	2.249e-09	9.8174e-16
	Worst	<b>0.00</b>	6.3429e-05	35.6743	5.085e-09	2.4431e-13
	Mean	<b>0.00</b>	1.0102e-05	9.3080	3.303e-09	1.9487e-14
	Median	<b>0.00</b>	2.0270e-06	6.9806	3.202e-09	6.3817e-15
	Std.	<b>0.00</b>	1.6927e-05	8.0720	7.442e-10	4.4955e-14
F <sub>5</sub>	Best	<b>0.122</b>	25.6273	27.3230	25.745	25.2273
	Worst	<b>8.171</b>	29.5430	49.5110	220.911	28.7294
	Mean	<b>2.337</b>	28.4422	29.9106	42.2647	26.9256
	Median	<b>0.721</b>	28.8115	29.0097	26.1443	27.1173
	Std.	<b>2.772</b>	0.7616	4.1508	45.4674	0.8418
F <sub>6</sub>	Best	1.9836e-07	2.0585	3.4070	<b>9.711e-18</b>	0.2466
	Worst	0.0220	4.7791	4.4435	<b>8.645e-16</b>	1.2619
	Mean	0.0021	3.6724	4.0360	<b>3.097e-17</b>	0.6376
	Median	1.9836e-07	3.5615	4.0572	<b>2.953e-17</b>	0.7452
	Std.	0.0056	0.6918	0.2954	<b>6.165e-18</b>	0.3353
F <sub>7</sub>	Best	<b>3.3002e-10</b>	6.7114e-04	0.0015	0.0061	1.5222e-04
	Worst	<b>1.2212e-04</b>	0.0036	0.0431	0.0462	0.0022
	Mean	<b>7.2800e-06</b>	0.0018	0.0116	0.0237	7.9976e-04
	Median	<b>3.3002e-10</b>	0.0018	0.0078	0.0222	7.0098e-04
	Std.	<b>2.4887e-05</b>	7.7268e-04	0.0101	0.0098	4.6287e-04

TABLE 6. Results comparison of multimodal test functions.

Fun	Index	ATSA	TSA	SCA	GSA	GWO
F <sub>8</sub>	Best	<b>-1.256e+04</b>	-7.892e+03	-5.299e+03	-3.627e+03	-8.817e+03
	Worst	<b>-1.256e+04</b>	-5.271e+03	-3.532e+03	-2.003e+03	-4.974e+03
	Mean	<b>-1.256e+04</b>	-6.616e+03	-4.076e+03	-2.782e+03	-6.252e+03
	Median	<b>-1.256e+04</b>	-6.611e+03	-3.972e+03	-2.746e+03	-6.227e+03
	Std.	<b>1.864</b>	599.2609	336.8249	365.4671	852.4634
F <sub>9</sub>	Best	<b>0.00</b>	77.7761	1.0560e-06	8.9546	0.00
	Worst	<b>0.00</b>	254.9883	51.4451	21.8891	10.0548
	Mean	<b>0.00</b>	151.4539	5.9694	15.6209	0.8853
	Median	<b>0.00</b>	149.6596	9.3391e-04	15.9193	0.00
	Std.	<b>0.00</b>	35.8717	12.2476	3.1043	2.4438
F <sub>10</sub>	Best	<b>8.8818e-16</b>	1.5099e-14	1.5579e-05	2.528e-09	1.1546e-14
	Worst	<b>8.8818e-16</b>	4.3125	20.2198	4.482e-09	2.2204e-14
	Mean	<b>8.8818e-16</b>	2.4095	14.3622	3.491e-09	1.5928e-14
	Median	<b>8.8818e-16</b>	2.9381	20.1275	3.476e-09	1.5099e-14
	Std.	<b>0.00</b>	1.3920	8.9778	5.153e-10	2.5861e-15
F <sub>11</sub>	Best	<b>0.00</b>	0.00	4.8381e-07	1.6952	0.00
	Worst	<b>0.00</b>	0.0159	0.7703	10.6642	0.0140
	Mean	<b>0.00</b>	0.0077	0.1368	4.2510	0.0014
	Median	<b>0.00</b>	0.0082	0.0032	3.5667	0.00
	Std.	<b>0.00</b>	0.0057	0.2218	2.0234	0.0041
F <sub>12</sub>	Best	<b>2.168e-06</b>	0.2738	0.2631	8.203e-02	0.0121
	Worst	<b>0.0022</b>	13.8088	5.6300	0.1037	0.0920
	Mean	<b>6.989e-04</b>	6.3735	0.9568	0.0198	0.0364
	Median	<b>5.342e-05</b>	6.7411	0.4964	1.3512	0.0329
	Std.	<b>6.822e-04</b>	3.4586	1.1497	0.0400	0.0201
F <sub>13</sub>	Best	2.6099e-05	1.7796	1.8452	<b>1.340e-18</b>	0.1006
	Worst	9.1819e-04	4.1077	22.5849	<b>0.0110</b>	1.0416
	Mean	<b>5.0093e-04</b>	2.8976	3.4211	7.324e-04	0.5280
	Median	5.1139e-04	2.8914	2.3552	<b>2.068e-18</b>	0.5238
	Std.	<b>4.2513e-04</b>	0.6436	3.9911	0.0028	0.2359

ATSA has inferior performance and alternative algorithm shown better performance [53].

According to the results of Wilcoxon’s rank sum test in Table 8, the pairwise comparison between ATSA and GSA reveals that in the optimization of 23 test functions, the new method has superior performance in 19 cases and has inferior performance in two cases. In addition, for F<sub>16</sub> and F<sub>20</sub>, both methods are statistically equivalent. Similarly, in the other pairwise comparison, for the majority of the test suite,

TABLE 7. Results comparison of fixed-dimension multimodal test functions.

Fun	Index	ATSA	TSA	SCA	GSA	GWO
F <sub>14</sub>	Best	<b>0.9980</b>	<b>0.9980</b>	<b>0.9980</b>	<b>0.9980</b>	<b>0.9980</b>
	Worst	<b>0.9980</b>	12.6705	2.9821	8.0858	12.6705
	Mean	<b>0.9980</b>	7.6657	1.1964	3.6212	4.1312
	Median	<b>0.9980</b>	10.7632	0.9980	3.0452	2.9821
	Std.	<b>1.477e-11</b>	4.8845	0.6054	2.1942	4.1443
F <sub>15</sub>	Best	<b>3.138e-04</b>	3.751e-04	3.4063e-04	0.0012	3.1749e-04
	Worst	<b>3.968e-04</b>	0.0566	0.0014	0.0118	0.0204
	Mean	<b>3.364e-04</b>	0.0043	8.5975e-04	0.0025	0.0044
	Median	<b>3.232e-04</b>	4.539e-04	7.3095e-04	0.0021	3.0754e-04
	Std.	<b>2.458e-05</b>	0.0116	3.8089e-04	0.0019	0.0081
F <sub>16</sub>	Best	<b>-1.0316</b>	-1.0316	<b>-1.0316</b>	<b>-1.0316</b>	<b>-1.0316</b>
	Worst	<b>-1.0316</b>	-1.0000	<b>-1.0316</b>	<b>-1.0316</b>	<b>-1.0316</b>
	Mean	<b>-1.0316</b>	-1.0306	<b>-1.0316</b>	<b>-1.0316</b>	<b>-1.0316</b>
	Median	<b>-1.0316</b>	-1.0316	<b>-1.0316</b>	<b>-1.0316</b>	<b>-1.0316</b>
	Std.	<b>1.859e-06</b>	0.0058	1.0395e-05	5.608e-05	<b>4.7385e-09</b>
F <sub>17</sub>	Best	<b>0.3979</b>	<b>0.3979</b>	<b>0.3979</b>	<b>0.3979</b>	<b>0.3979</b>
	Worst	0.4011	0.3980	0.3992	<b>0.3979</b>	<b>0.3979</b>
	Mean	0.3987	0.3979	0.3982	<b>0.3979</b>	<b>0.3979</b>
	Median	0.3985	0.3979	0.3981	<b>0.3979</b>	<b>0.3979</b>
	Std.	7.939e-04	1.371e-05	3.4881e-04	0	1.1055e-06
F <sub>18</sub>	Best	<b>3.000</b>	<b>3.000</b>	<b>3.000</b>	<b>3.000</b>	<b>3.000</b>
	Worst	3.005	84.00	<b>3.000</b>	<b>3.000</b>	<b>3.000</b>
	Mean	3.002	5.700	<b>3.000</b>	<b>3.000</b>	<b>3.000</b>
	Median	3.002	3.000	<b>3.000</b>	<b>3.000</b>	<b>3.000</b>
	Std.	1.702e-05	14.7885	5.3498e-06	<b>1.592e-15</b>	9.5052e-06
F <sub>19</sub>	Best	<b>-3.8628</b>	<b>-3.8628</b>	-3.8625	<b>-3.8628</b>	<b>-3.8628</b>
	Worst	<b>-3.8628</b>	-3.8549	-3.8539	<b>-3.8628</b>	-3.8549
	Mean	<b>-3.8628</b>	-3.8625	-3.8560	<b>-3.8628</b>	-3.8620
	Median	<b>-3.8628</b>	-3.8628	-3.8548	<b>-3.8628</b>	-3.8628
	Std.	<b>1.362e-16</b>	0.0014	0.0029	2.479e-05	0.0022
F <sub>20</sub>	Best	<b>-3.3220</b>	-3.3216	-3.1918	<b>-3.3220</b>	<b>-3.3220</b>
	Worst	<b>-3.3220</b>	-3.0885	-2.0488	<b>-3.3220</b>	-3.0292
	Mean	<b>-3.3220</b>	-3.2538	-3.0155	<b>-3.3220</b>	-3.2493
	Median	<b>-3.3220</b>	-3.2028	-3.0139	<b>-3.3220</b>	-3.2625
	Std.	<b>1.355e-16</b>	0.0671	0.1974	<b>1.355e-15</b>	0.0821
F <sub>21</sub>	Best	<b>-10.1532</b>	-10.1361	-8.1370	<b>-10.1532</b>	-10.1531
	Worst	<b>-10.1532</b>	-2.6669	-0.8802	-2.6829	-5.0999
	Mean	<b>-10.1532</b>	-7.2879	-4.3187	-6.3969	-9.4790
	Median	<b>-10.1532</b>	-7.4198	-4.9053	-3.9547	-10.1526
	Std.	<b>2.499e-07</b>	2.8594	2.0785	3.5901	1.7469
F <sub>22</sub>	Best	<b>-10.4028</b>	-10.3812	-9.0513	-10.4009	-10.4029
	Worst	<b>-10.4028</b>	-2.7427	-0.9074	-10.4029	-5.0877
	Mean	<b>-10.4028</b>	-7.8325	-5.4154	-10.4029	-10.2253
	Median	<b>-10.4028</b>	-10.2554	-5.0380	-10.4028	-10.4025
	Std.	<b>5.420e-15</b>	3.1843	1.7315	4.664e-06	0.9703
F <sub>23</sub>	Best	<b>-10.5363</b>	-10.5193	-9.3851	-10.5364	<b>-10.5363</b>
	Worst	<b>-10.5362</b>	-1.6752	-3.2531	-10.5364	-10.5354
	Mean	<b>-10.5363</b>	-7.6730	-5.2925	-10.5364	-10.5359
	Median	<b>-10.5363</b>	-10.4114	-5.0398	-10.5364	-10.5360
	Std.	<b>2.485e-05</b>	3.7585	1.0982	1.836e-15	2.5855e-04

ATSA provides better results. Therefore, the nonparametric statistical analysis proves that ATSA generated significantly better solutions and, comparatively, has superior performance over the other algorithms.

As the results show, the ATSA is capable of conducting a full investigation of the search area and promptly identifying the most promising position. Based on the findings, it can be inferred that ATSA outperforms the original algorithm as well as alternative optimization methods.

## VI. MODEL APPLICATION

In this section, the optimum design of an interior spread footing in dry sand is conducted using the proposed ATSA by considering two objective functions: CO<sub>2</sub> emission and construction cost. This problem has been solved previously by Camp and Assadollahi [45] using a hybrid big bang-big crunch (BB-BC) algorithm. The input parameters for the case study are given in Table 9.

The problem is solved by the presented procedure for both the cost and CO<sub>2</sub> objective functions. In order to verify the efficiency of the proposed ATSA method, the analysis

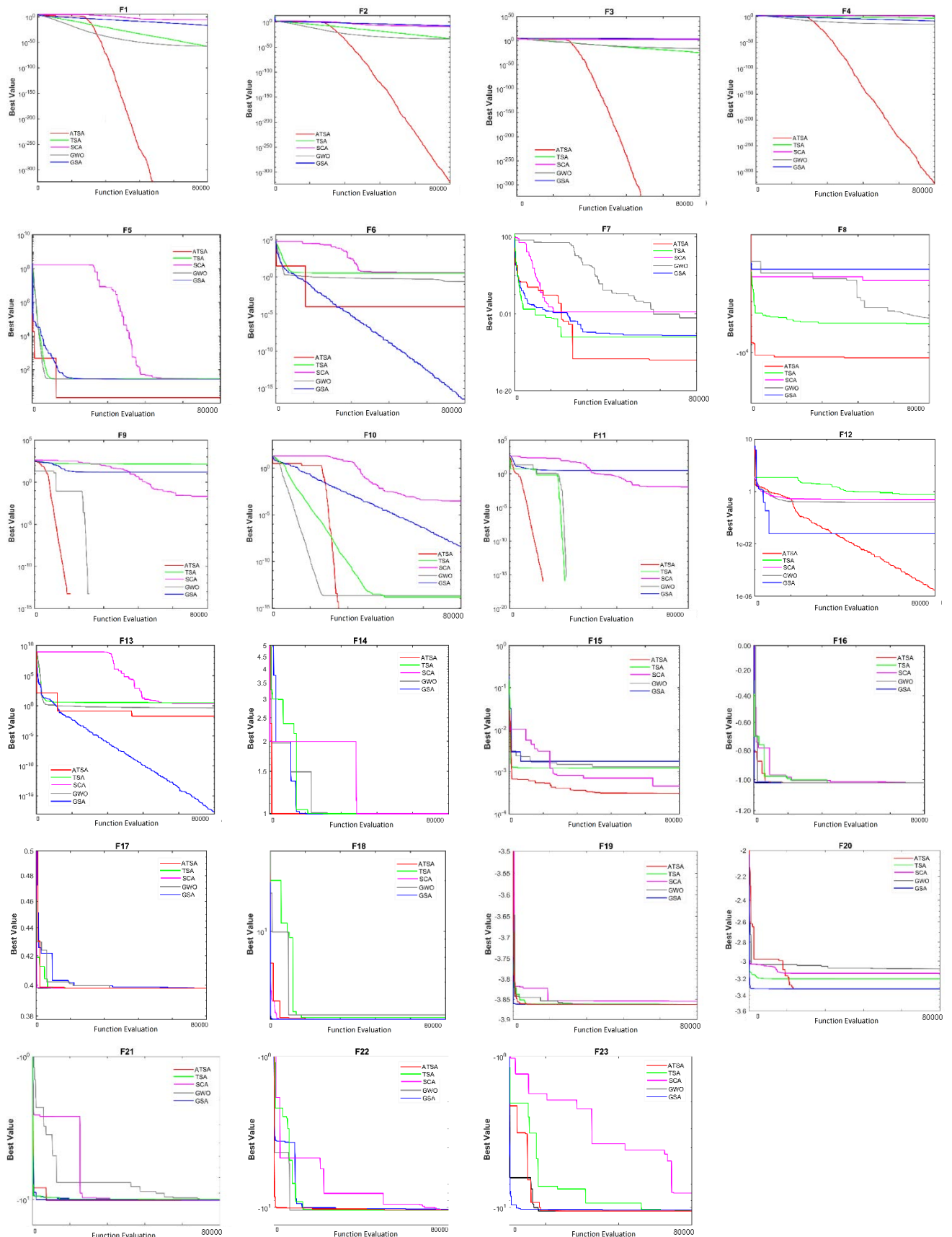


FIGURE 3. Convergence curve of test functions.

TABLE 8. Results of Wilcoxon’s rank sum test.

Fun	Wilcoxon test Parameters	ATSA vs TSA	ATSA vs GSA	ATSA vs SCA	ATSA vs GWO
F1	p- value	1.7344E-06	1.7344E-06	1.7344E-06	1.7344E-06
	R+	465	465	465	465
	R-	0	0	0	0
	Winner	ATSA	ATSA	ATSA	ATSA
F2	p- value	1.7344E-06	1.7344E-06	1.7344E-06	1.7344E-06
	R+	465	465	465	465
	R-	0	0	0	0
	Winner	ATSA	ATSA	ATSA	ATSA
F3	p- value	1.7344E-06	1.7344E-06	1.7344E-06	1.7344E-06
	R+	465	465	465	465
	R-	0	0	0	0
	Winner	ATSA	ATSA	ATSA	ATSA
F4	p- value	1.7344E-06	1.7344E-06	1.7344E-06	1.7344E-06
	R+	465	465	465	465
	R-	0	0	0	0
	Winner	ATSA	ATSA	ATSA	ATSA
F5	p- value	1.7344E-06	1.7344E-06	1.7344E-06	1.7344E-06
	R+	465	465	465	465
	R-	0	0	0	0
	Winner	ATSA	ATSA	ATSA	ATSA
F6	p- value	1.7344E-06	7.4523E-7	1.7344E-06	2.353E-06
	R+	465	465	462	465
	R-	0	465	0	3
	Winner	ATSA	GSA	ATSA	ATSA
F7	p- value	1.7344E-06	1.7344E-06	1.7344E-06	1.7344E-06
	R+	465	465	465	465
	R-	0	0	0	0
	Winner	ATSA	ATSA	ATSA	ATSA
F8	p- value	1.7344E-06	1.7344E-06	1.7344E-06	1.7344E-06
	R+	465	465	465	465
	R-	0	0	0	0
	Winner	ATSA	ATSA	ATSA	ATSA
F9	p- value	1.7344E-06	1.7344E-06	1.7344E-06	0.02
	R+	465	465	465	21
	R-	0	0	0	0
	Winner	ATSA	ATSA	ATSA	ATSA
F10	p- value	1.73E-06	1.73E-06	1.73E-06	1.73E-06
	R+	465	465	465	465
	R-	0	0	0	0
	Winner	ATSA	ATSA	ATSA	ATSA
F11	p- value	1.473E-03	1.73E-06	1.73E-06	0.068
	R+	91	465	465	10
	R-	0	0	0	0
	Winner	ATSA	ATSA	ATSA	N.A
F12	p- value	1.73E-06	1.73E-06	1.73E-06	1.73E-06
	R+	465	465	465	465
	R-	0	0	0	0
	Winner	ATSA	ATSA	ATSA	ATSA
F13	p- value	1.73E-06	3.74E-04	1.73E-06	1.73E-06
	R+	465	66	465	465
	R-	0	399	0	0
	Winner	ATSA	GSA	ATSA	ATSA
F14	p- value	4.81E-06	1.73E-06	2.56E-06	3.22E-04
	R+	403	465	435	152
	R-	3	0	0	1
	Winner	ATSA	ATSA	ATSA	ATSA
F15	p- value	0.006	1.73E-06	2.35E-06	0.393
	R+	366	465	462	274
	R-	99	0	3	191
	Winner	ATSA	ATSA	ATSA	N.A
F16	p- value	0.132	0.059	0.371	1.59E-06
	R+	50	304	276	0
	R-	415	161	189	465
	Winner	N.A	N.A	N.A	GWO
F17	p- value	1.73E-06	1.37E-06	3.18E-06	1.73E-06
	R+	465	465	465	0
	R-	0	0	0	465
	Winner	ATSA	ATSA	ATSA	GWO
F18	p- value	3.11E-05	1.08E-06	1.73E-06	1.73E-06
	R+	30	0	0	0
	R-	435	465	465	465
	Winner	ATSA	GSA	SCA	GWO
F19	p- value	1.73E-06	8.38E-08	1.73E-06	1.73E-06
	R+	465	465	465	465
	R-	0	0	0	0
	Winner	ATSA	ATSA	ATSA	ATSA
F20	p- value	1.73E-06	0.894	1.73E-06	1.73E-06
	R+	465	229	465	465
	R-	0	226	0	0
	Winner	ATSA	N.A	ATSA	ATSA
F21	p- value	1.73E-06	0.046	1.73E-06	1.73E-06
	R+	465	329	465	465
	R-	0	136	0	0
	Winner	ATSA	ATSA	ATSA	ATSA
F22	p- value	1.73E-06	1.44E-07	1.73E-06	2.13E-06
	R+	465	465	465	463
	R-	0	0	0	2
	Winner	ATSA	ATSA	ATSA	ATSA
F23	p- value	1.73E-06	1.46E-05	1.73E-06	3.51E-6
	R+	465	435	465	458
	R-	0	30	0	7
	Winner	ATSA	ATSA	ATSA	ATSA
Total	Superior /Inferior/N.A	22/0/1	19/2/2	21/1/1	18/3/2

TABLE 9. Input parameters for the case study [45].

Parameter	Unit	Symbol	Value
Effective friction angle of base soil	degree	$\phi$	35
Unit weight of base soil	kN/m <sup>3</sup>	$\gamma_s$	18.5
Young’s modulus	MPa	$E$	50
Poisson’s ratio	–	$\nu$	0.3
Vertical load	kN	$P$	3000
Moment	kN-m	$M$	0.0
Concrete cover	cm	$d_c$	7.0
Over excavation length	m	$L_0$	0.3
Over excavation width	m	$B_0$	0.3
Yield strength of reinforcing steel	MPa	$f_y$	400
Compressive strength of concrete	MPa	$f_c$	30
Factor of safety for bearing capacity	–	$FS$	3.0
Allowable settlement of footing	mm	$\delta_{all}$	25

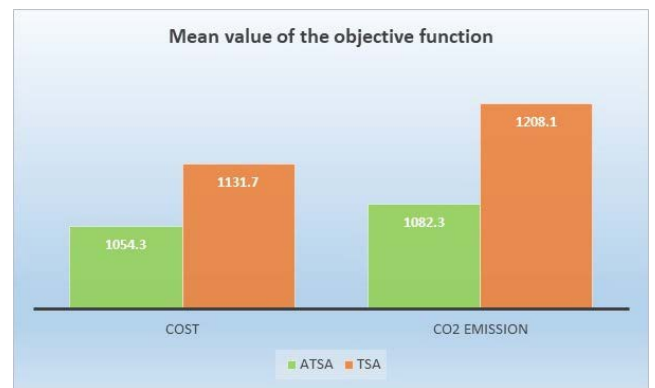


FIGURE 4. Average values of the objective functions.

results are compared with the standard TSA as well as BB-BC algorithms [45]. In this experiment, the maximum number of function evaluations is considered equal to 50,000. Both the TSA and ATSA algorithms are run 30 times, and the best results of the analyses for the minimum cost and minimum CO<sub>2</sub> emission obtained by each method are presented in Table 10.

The findings presented in Table 10 show that the optimum design evaluated by the proposed ATSA algorithm is lower than those evaluated by standard TSA and BB-BC techniques. According to the result, the best price obtained by ATSA is 1046.8\$, which is almost 4.8% lower than the best price calculated by TSA and 3.7% lower than the BB-BC’s result, which means the new method could provide a cheaper design. In addition, the best value of the CO<sub>2</sub> objective function calculated by the new algorithm is almost 7.2% and 4.2% lower than those evaluated by the TSA and BB-BC methods, respectively.

TABLE 10. Optimization result for spread footing optimization.

Design variable	Unit	Optimum Value					
		Best Cost Results			Best CO <sub>2</sub> Emission Results		
		ATSA	TSA	BB-BC[45]	ATSA	TSA	BB-BC[45]
$X_1$	m	2.322	2.268	2.3	2.167	2.488	2.10
$X_2$	m	1.623	1.659	1.86	1.666	1.581	2.09
$X_3$	m	0.498	0.498	0.6	0.494	0.502	0.6
$X_4$	m	1.623	2.0	1.3	1.665	1.58	1.26
$X_5$	cm <sup>2</sup>	44	42	-	39	48	-
$X_6$	cm <sup>2</sup>	23	24	-	25	22	-
Best Value of the Objective Function		1046.8\$	1099.6\$	1086\$	1072.4 kg	1156.3 kg	1119.53

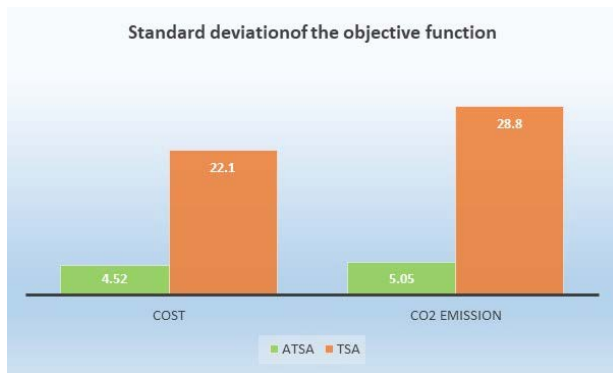


FIGURE 5. Standard deviation of the results.

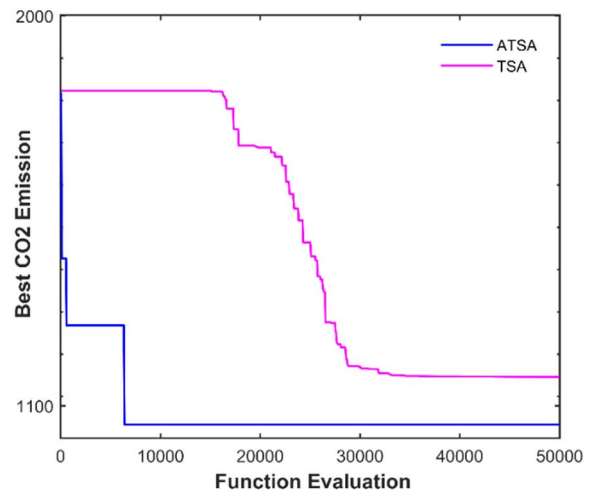


FIGURE 7. Convergence of TSA and ATSA for CO<sub>2</sub> function.

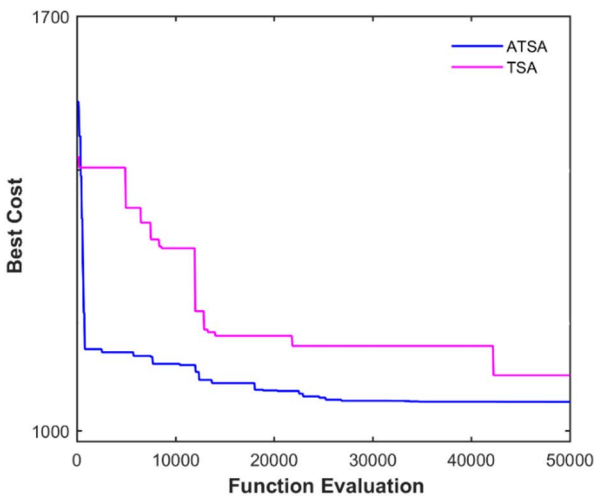


FIGURE 6. Convergence of TSA and ATSA for cost function.

Figures 4 and 5 illustrate the average and standard deviation of the cost and CO<sub>2</sub> objective functions from 30 different runs, respectively. Based on these findings, the mean values of the objective functions acquired by ATSA are lower than

those obtained by TSA. Furthermore, the standard deviation of the ATSA results is much smaller than that of the original method, demonstrating that the ATSA significantly improves the TSA’s instability.

The convergence progress curves of ATSA for cost and CO<sub>2</sub> objective functions are compared to those of TSA in Figs 6 and 7. As shown in these figures, the ATSA is capable of exploring the search space extensively and identifying the most promising region in fewer iterations because of its effective modifications. From the above results, it can be inferred that ATSA outperforms the original algorithm and the findings confirm the effectiveness of the new algorithm for optimization of spread foundations.

In the last part of this section, a sensitivity analysis is carried out to investigate the effects of soil parameters on the spread foundation design. Ground conditions and soil characteristics influence geotechnical engineering designs. As a result, a comprehensive site study is required to determine the ground conditions and design input parameters. In order



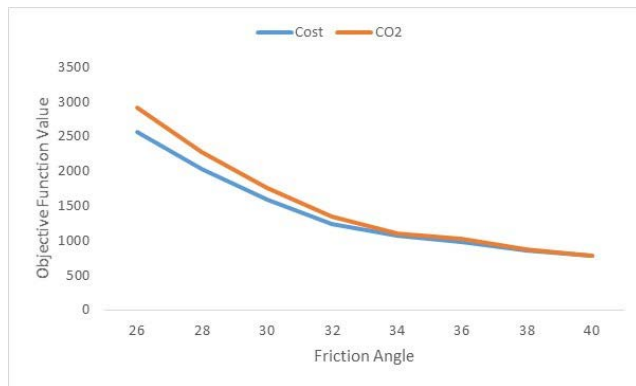


FIGURE 8. Effects of  $\phi$  variation on the cost and CO<sub>2</sub> emission.

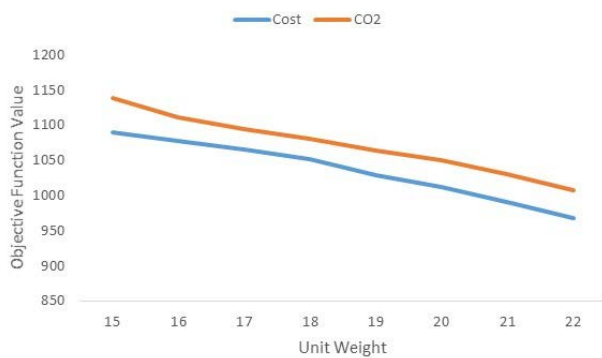


FIGURE 9. Effects of  $\gamma$  variation on the cost and CO<sub>2</sub> emission.

to explore the effect of soil parameters on the final design, the total construction cost and CO<sub>2</sub> emission of the foundation are computed by different values of effective friction angle ( $\phi$ ) and unit weight of soil ( $\gamma$ ). Figure 8 shows the low-cost and low-CO<sub>2</sub> emission designs of a foundation for different values of  $\phi$  as the internal friction angle of the soil varies from 26 to 40 degrees. As shown in Figure 8, Over this range, the construction cost and CO<sub>2</sub> emissions decrease drastically as the friction angle of the soil ( $\phi$ ) increases. However, if  $\phi$  becomes greater than 34, the intensity of variation will be reduced.

In the second stage, the total construction cost and CO<sub>2</sub> emissions are obtained using different values of unit weight of soil while the other properties are kept fixed. The results are shown graphically in Figure 9 and indicate that increasing the soil's unit weight ( $\gamma$ ) from 15 to 22 KN/m<sup>3</sup> reduces the total price and CO<sub>2</sub> emissions by nearly 12%.

The findings show that variations in effective friction angle have the greatest effects on total cost and CO<sub>2</sub> emissions, and that this parameter is critical in the optimal design of spread foundation. In other words, this parameter should be measured as accurately as possible during the site investigation.

## VII. CONCLUSION

In this paper, two main contributions are presented: (i) a novel adaptive version of the tunicate swarm algorithm called ATSA is introduced and verified using a set of

23 mathematical test functions of the well-known CEC 2017; and (ii) the proposed ATSA is applied for the low-cost and low-CO<sub>2</sub> emission design of shallow foundations. The proposed method has the potential to increase the TSA's exploration ability while also preventing it from becoming trapped in a local minima location. The new method's performance is evaluated using a combination of unimodal and multimodal benchmark functions. According to the results and findings, In terms of finding the global solution for most unimodal and multimodal functions, ATSA outperforms standard TSA as well as other approaches, In the next step, the proposed ATSA is applied to the optimum design of the shallow foundation. The performance of the new algorithm for the minimization of construction costs and CO<sub>2</sub> emissions of the foundation is investigated by considering a case study from the literature. When compared to existing algorithms, the findings indicate that the newly proposed method is quite robust and efficient for optimum design of spread foundations. Finally, a sensitivity analysis reveals the importance of the internal friction angle of the soil on the final construction cost and CO<sub>2</sub> emissions.

There are several potential applications and research directions that can be recommended for future work. Many engineering problems can be solved using the proposed algorithm, including structural optimization, damping controller design for power system oscillations, image processing, pipe routing design, optimal power flow problems, resource scheduling, and neural network training.

Like all stochastic optimization techniques, one of the limitations of the proposed ATSA is that new optimizers may be developed in the future that will perform better than ATSA in some real applications. Additionally, due to the stochastic nature of the ATSA, it cannot be guaranteed that the solutions obtained using the ATSA for optimization problems are exactly equal to the global optimum for all optimization problems.

## REFERENCES

- [1] J. Kennedy and R. Eberhart, "Particle swarm optimization," in *Proc. Int. Conf. Neural Netw. (ICNN)*, Perth, WA, Australia, 1995, pp. 1942–1948.
- [2] M. Dorigo and G. Di Caro, "Ant colony optimization: A new metaheuristic," in *Proc. Congr. Evol. Comput. (CEC)*, vol. 2, Jul. 1999, pp. 1470–1477.
- [3] Z. W. Geem, J. H. Kim, and G. V. Loganathan, "A new heuristic optimization algorithm: Harmony search," *J. Simul.*, vol. 76, no. 2, pp. 60–68, Feb. 2001.
- [4] X. S. Yang, "Firefly algorithms for multimodal optimization," in *Proc. Int. Symp. Stochastic Algorithms*, in Lecture Notes in Computer Science, vol. 5792, 2009, pp. 169–178.
- [5] E. Rashedi, H. Nezamabadi-Pour, and S. Saryzadi, "GSA: A gravitational search algorithm," *J. Inf. Sci.*, vol. 179, no. 13, pp. 2232–2248, 2009.
- [6] S. Mirjalili, "SCA: A sine cosine algorithm for solving optimization problems," *Knowl.-Based Syst.*, vol. 96, pp. 120–133, Mar. 2016.
- [7] A. Askarzadeh, "A novel metaheuristic method for solving constrained engineering optimization problems: Crow search algorithm," *Comput. Struct.*, vol. 169, pp. 1–12, Jun. 2016.
- [8] G. Dhiman and V. Kumar, "Spotted hyena optimizer: A novel bio-inspired based metaheuristic technique for engineering applications," *Adv. Eng. Softw.*, vol. 114, pp. 48–70, Dec. 2017.
- [9] A. A. Heidari, S. Mirjalili, H. Faris, I. Aljarah, M. Mafarja, and H. Chen, "Harris hawks optimization: Algorithm and applications," *Future Gener. Comput. Syst.*, vol. 97, pp. 849–872, Aug. 2019.

- [10] G. Dhiman and V. Kumar, "Emperor penguin optimizer: A bio-inspired algorithm for engineering problems," *Knowl. Based Syst.*, vol. 159, pp. 20–50, Nov. 2018.
- [11] M. S. Braik, "Chameleon swarm algorithm: A bio-inspired optimizer for solving engineering design problems," *Expert Syst. Appl.*, vol. 174, Jul. 2021, Art. no. 114685.
- [12] G. Dhiman and A. Kaur, "STOA: A bio-inspired based optimization algorithm for industrial engineering problems," *Eng. Appl. Artif. Intell.*, vol. 82, pp. 148–174, Jun. 2019.
- [13] I. Naruei, F. Keynia, and A. Sabbagh Molahosseini, "Hunter-Prey optimization: Algorithm and applications," *Soft Comput.*, vol. 26, no. 3, pp. 1279–1314, Feb. 2022.
- [14] G. Dhiman, M. Garg, A. Nagar, V. Kumar, and M. Dehghani, "A novel algorithm for global optimization: Rat swarm optimizer," *J. Ambient Intell. Humanized Comput.*, vol. 12, pp. 1–26, Oct. 2020.
- [15] G. Dhiman, "ESA: A hybrid bio-inspired metaheuristic optimization approach for engineering problems," *Eng. Comput.*, vol. 37, no. 1, pp. 323–353, Jan. 2021.
- [16] M. Eslami, H. Shareef, A. Mohamed, and M. Khajehzadeh, "Optimal location of PSS using improved PSO with chaotic sequence," in *Proc. Int. Conf. Electr., Control Comput. Eng. (InECCE)*, Jun. 2011, pp. 253–258.
- [17] H. Bingol and B. Alatas, "Chaotic league championship algorithms," *Arabian J. Sci. Eng.*, vol. 41, no. 12, pp. 5123–5147, Dec. 2016.
- [18] A. Kaveh, M. Kalateh-Ahani, and M. Fahimi-Farzam, "Life-cycle cost optimization of steel moment-frame structures: Performance-based seismic design approach," *Earthquake Struct.*, vol. 7, no. 3, pp. 94–271, 2014.
- [19] G. Dhiman, D. Oliva, A. Kaur, K. K. Singh, S. Vimal, A. Sharma, and K. Cengiz, "BEPO: A novel binary emperor penguin optimizer for automatic feature selection," *Knowl.-Based Syst.*, vol. 211, Jan. 2021, Art. no. 106560.
- [20] S. Li and L. Wu, "An improved salp swarm algorithm for locating critical slip surface of slopes," *Arabian J. Geosci.*, vol. 14, no. 5, pp. 1–11, Mar. 2021.
- [21] R. Temur, "Optimum design of cantilever retaining walls under seismic loads using a hybrid TLBO algorithm," *Geomechan. Eng.*, vol. 24, no. 3, pp. 237–251, 2021.
- [22] A. Bardhan, A. GuhaRay, S. Gupta, B. Pradhan, and C. Gokceoglu, "A novel integrated approach of ELM and modified equilibrium optimizer for predicting soil compression index of subgrade layer of dedicated freight corridor," *Transp. Geotechnics*, vol. 32, Jan. 2022, Art. no. 100678.
- [23] C. M. Chan, L. M. Zhang, and J. T. Ng, "Optimization of pile groups using hybrid genetic algorithms," *J. Geotech. Geoenviron. Eng.*, vol. 135, no. 4, pp. 497–505, Apr. 2009.
- [24] H. Bingol and B. Alatas, "Chaos based optics inspired optimization algorithms as global solution search approach," *Chaos, Solitons Fractals*, vol. 141, Dec. 2020, Art. no. 110434.
- [25] R. Kumar and G. Dhiman, "A comparative study of fuzzy optimization through fuzzy number," *Int. J. Mod. Res.*, vol. 1, no. 1, pp. 1–14, 2021.
- [26] M. Khajehzadeh, M. R. Taha, and M. Eslami, "Multi-objective optimization of foundation using global-local gravitational search algorithm," *Struct. Eng. Mech., Int. J.*, vol. 50, no. 3, pp. 257–273, May 2014.
- [27] Y. Wang and F. H. Kulhawy, "Economic design optimization of foundations," *J. Geotechnical Geoenviron. Eng.*, vol. 134, no. 8, pp. 1097–1105, Aug. 2008.
- [28] S. M. Nigdeli, G. Bekdaş, and X.-S. Yang, "Metaheuristic optimization of reinforced concrete footings," *KSCE J. Civil Eng.*, vol. 22, no. 11, pp. 4555–4563, Nov. 2018.
- [29] A. H. Gandomi and A. R. Kashani, "Construction cost minimization of shallow foundation using recent swarm intelligence techniques," *IEEE Trans. Ind. Informat.*, vol. 14, no. 3, pp. 1099–1106, Mar. 2018.
- [30] A. R. Kashani, M. Gandomi, C. V. Camp, and A. H. Gandomi, "Optimum design of shallow foundation using evolutionary algorithms," *Soft Comput.*, vol. 24, no. 9, pp. 6809–6833, May 2020.
- [31] V. Yepes, F. Gonzalez-Vidosa, J. Alcalá, and P. Villalba, "CO<sub>2</sub>-optimization design of reinforced concrete retaining walls based on a VNS-threshold acceptance strategy," *J. Comput. Civil Eng.*, vol. 26, no. 3, pp. 378–386, May 2012.
- [32] I. Paya-Zaforteza, V. Yepes, A. Hospitaler, and F. González-Vidosa, "CO<sub>2</sub>-optimization of reinforced concrete frames by simulated annealing," *Eng. Struct.*, vol. 31, no. 7, pp. 1501–1508, Jul. 2009.
- [33] V. Yepes, J. V. Martí, and T. García-Segura, "Cost and CO<sub>2</sub> emission optimization of precast-prestressed concrete U-beam road bridges by a hybrid glowworm swarm algorithm," *Autom. Construct.*, vol. 49, pp. 123–134, Jan. 2015.
- [34] M. Khajehzadeh, M. R. Taha, and M. Eslami, "Multi-objective optimization of retaining walls using hybrid adaptive gravitational search algorithm," *Civil Eng. Environ. Syst.*, vol. 31, no. 3, pp. 229–242, Jul. 2014.
- [35] S. Kaur, L. K. Awasthi, A. L. Sangal, and G. Dhiman, "Tunicate swarm algorithm: A new bio-inspired based metaheuristic paradigm for global optimization," *Eng. Appl. Artif. Intell.*, vol. 90, Apr. 2020, Art. no. 103541.
- [36] A. Sharma, A. Dasgotra, S. K. Tiwari, A. Sharma, V. Jatly, and B. Azzopardi, "Parameter extraction of photovoltaic module using tunicate swarm algorithm," *Electronics*, vol. 10, no. 8, p. 878, Apr. 2021.
- [37] L.-L. Li, Z.-F. Liu, M.-L. Tseng, S.-J. Zheng, and M. K. Lim, "Improved tunicate swarm algorithm: Solving the dynamic economic emission dispatch problems," *Appl. Soft Comput.*, vol. 108, Sep. 2021, Art. no. 107504.
- [38] T. Fetouh and A. M. Elsayed, "Optimal control and operation of fully automated distribution networks using improved tunicate swarm intelligent algorithm," *IEEE Access*, vol. 8, pp. 129689–129708, 2020.
- [39] R. M. Rizk-Allah, O. Saleh, E. A. Hagag, and A. A. A. Mousa, "Enhanced tunicate swarm algorithm for solving large-scale nonlinear optimization problems," *Int. J. Comput. Intell. Syst.*, vol. 14, no. 1, pp. 1–24, Dec. 2021.
- [40] F. N. Al-Wesabi, M. Obayya, A. M. Hilal, O. Castillo, D. Gupta, and A. Khanna, "Multi-objective quantum tunicate swarm optimization with deep learning model for intelligent dystrophia diagnosis," *Soft Comput.*, early access, pp. 1–16, Jan. 2022, doi: 10.1007/s00500-021-06620-5.
- [41] M. Mansoor, A. F. Mirza, F. Long, and Q. Ling, "An intelligent tunicate swarm algorithm based MPPT control strategy for multiple configurations of PV systems under partial shading conditions," *Adv. Theory Simul.*, vol. 4, no. 12, 2021, Art. no. 2100246.
- [42] M. Khajehzadeh, S. Keawsawong, P. Sarir, and D. K. Khailany, "Seismic analysis of earth slope using a novel sequential hybrid optimization algorithm," *Periodica Polytechnica Civil Eng.*, vol. 66, pp. 355–366, 2022.
- [43] E. H. Houssein, B. E.-D. Helmy, A. A. Elgar, D. S. Abdelminaam, and H. Shaban, "An improved tunicate swarm algorithm for global optimization and image segmentation," *IEEE Access*, vol. 9, pp. 56066–56092, 2021.
- [44] J. Wang, S. Wang, and Z. Li, "Wind speed deterministic forecasting and probabilistic interval forecasting approach based on deep learning, modified tunicate swarm algorithm, and quantile regression," *Renew. Energy*, vol. 179, pp. 1246–1261, Dec. 2021.
- [45] C. V. Camp and A. Assadollahi, "CO<sub>2</sub> and cost optimization of reinforced concrete footings using a hybrid big bang-big crunch algorithm," *Struct. Multidisciplinary Optim.*, vol. 48, no. 2, pp. 411–426, Aug. 2013.
- [46] H. G. Poulos and E. H. Davis, *Elastic Solutions for Soil and Rock Mechanics*. New York, NY, USA: Wiley, 1974.
- [47] *318-05. Building Code Requirements for Structural Concrete and Commentary*, Amer. Concrete Inst. Int., Farmington Hills, MI, USA 2005.
- [48] N. K. Dandu, "Optimization of benchmark functions using chemical reaction optimization," M.S. thesis, Dept. Comput. Sci., North Dakota State Univ. Agricult. Appl. Sci., Fargo, ND, USA, 2013.
- [49] Q. Askari, I. Younas, and M. Saeed, "Political optimizer: A novel socio-inspired meta-heuristic for global optimization," *Knowl.-Based Syst.*, vol. 195, May 2020, Art. no. 105709.
- [50] S. Mirjalili, S. M. Mirjalili, and A. Lewis, "Grey wolf optimizer," *Adv. Eng. Softw.*, vol. 69, pp. 46–61, Mar. 2014.
- [51] J. Derrac, S. García, D. Molina, and F. Herrera, "A practical tutorial on the use of nonparametric statistical tests as a methodology for comparing evolutionary and swarm intelligence algorithms," *Swarm Evol. Comput.*, vol. 1, no. 1, pp. 3–18, Mar. 2011.
- [52] *SPSS-Tutorials, Version 23*, Int. Bus. Mach., New York, NY, USA, 2016.
- [53] M. Toz, "Chaos-based vortex search algorithm for solving inverse kinematics problem of serial robot manipulators with offset wrist," *Appl. Soft Comput.*, vol. 89, Apr. 2020, Art. no. 106074.



**AMIRBAHADOR ARABALI** received the Ph.D. degree in civil engineering—structure from the Azad University of Central Tehran, Iran, in 2021. His research interests include reinforced and pre-stressed structures and concrete engineering using advanced or recycled materials, steel, and composite structures.



**MOHAMMAD KHAJEHZADEH** received the bachelor's and master's degrees in civil engineering from the Islamic Azad University of Kerman, Iran, in 2001 and 2004, respectively, and the Ph.D. degree in geotechnical engineering from University Kebangsaan Malaysia, in 2011. He is currently an Assistant Professor with the Civil Engineering Department, Islamic Azad University of Anar. He has published more than 40 journal articles and two books. His research interests include geotechnical analysis, artificial intelligence, and application of optimization in field of geotechnical engineering problems.



**SURAPARB KEAWSAWASVONG** received the B.Eng. degree (Hons.) in civil engineering from Thammasat University, Thailand, in 2013, and the M.Eng. and Ph.D. degrees in civil engineering from Chulalongkorn University, Thailand, in 2015 and 2019, respectively. He is currently a Lecturer at the Department of Civil Engineering, Thammasat University. His research interests include stability analysis in geotechnical engineering, solid mechanics, optimization, and finite element analysis.



**ADIL HUSSEIN MOHAMMED** received the B.Sc. degree in electrical and electronic engineering and the M.Sc. degree in communication engineering. He is currently an Assistant Lecturer (Full) and teaching at the Department of Communication and Computer, Cihan University-Erbil, Kurdistan Region, Iraq.



**BASEEM KHAN** (Senior Member, IEEE) received the B.Eng. degree in electrical engineering from Rajiv Gandhi Technological University, Bhopal, India, in 2008, and the M.Tech. and D.Phil. degrees in electrical engineering from the Maulana Azad National Institute of Technology, Bhopal, in 2010 and 2014, respectively. He is currently working as a Faculty Member at Hawassa University, Ethiopia. He has published more than 100 research articles in well reputable research journals, including IEEE TRANSACTION, IEEE ACCESS, *Computer and Electrical Engineering* (Elsevier), *IET GTD*, *IET RPG*, and *IET Power Electronics*. Further, he has published, authored, and edited books with Wiley, CRC Press, and Elsevier. His research interests include power system restructuring, power system planning, smart grid technologies, meta-heuristic optimization techniques, reliability analysis of renewable energy systems, power quality analysis, and renewable energy integration.

...